J/ψ azimuthal anisotropy in Au+Au collisions at $\sqrt{s_{NN}}$ = 200 GeV

Chensheng Zhou(for the STAR Collaboration)

Shanghai Institute of Applied Physics, Chinese Academy of Sciences, Shanghai 201800, China
and
Brookhaven National Laboratory, Upton, NY 11973, USA

Abstract.

The study of J/ψ azimuthal anisotropy allows for a disentanglement of various production mechanisms and possibly an access to charm quark azimuthal anisotropy. J/ψ meson produced from direct pQCD processes have little azimuthal anisotropy due to the lack of collectivity or azimuthal preference of initial emitting, while J/ψ meson produced from recombination of charm quarks in the medium are expected to inherit the azimuthal anisotropy of the constituent charm quarks. We present measurements of J/ψ azimuthal anisotropy, with J/ψ reconstructed via the di-electron channel, as a function of transverse momentum in Au+Au collisions at $\sqrt{s_{NN}}$ = 200 GeV. This analysis is carried out with data taken by the STAR experiment during RHIC operation in year 2011. Combined with the published results using 2010 data, the updated results provide further support to the conclusion that J/ψ production above 2 GeV/c is unlikely to be dominated by regeneration of fully thermalized charm quarks.

1. Introduction

Mounting evidences [1–6] have supported that a quark-gluon plasma (QGP) has been produced in ultra-relativistic heavy-ion collisions at the Relativistic Heavy-Ion Collider (RHIC) at Brookhaven National Laboratory, as well as at the Large Hadron Collider at CERN. Yet the property of QGP is still under intensive investigations. Out of many probes that are used to study QGP, charm quark is a unique one [7, 8]. Charm quarks are produced in early steps of the heavy-ion collisions and experience the entire evolution of the QGP. Charm quarks have large masses, which make them a genuine hard probe even at low p_T. Sizable collective motion of charm quarks is an indication of early thermalization, measurement of which is useful for understanding the dynamics responsible for fast thermalization at RHIC. The measurement of J/ψ azimuthal anisotropy, especially its second Fourier coefficient v_2 (elliptic flow) [9], can be used to infer the relative contributions from different production sources [10, 11], as they each give its own characteristic pattern in terms of v_2 magnitudes and p_T dependence. In that sense, J/ψ v_2 is a unique probe for testing production mechanisms and useful for constraining models.

There are many models trying to describe the experimental results of J/ψ v_2. The one that is based on the coalescence of fully thermalized charm quarks [7] gives large v_2, and its increase with p_T starts at relatively large p_T. In the model that considers the direct pQCD production [10], as heavy quarks are expected to thermalize much more slowly than light quarks, the phase space distribution of massive J/ψ is governed by transport rather than kinetic equation, which produces limited v_2 due to the leakage effect. In a recent work, the J/ψ

v_2 is studied under the influence of external magnetic field [12]. With the presence of strong magnetic field, generated early and short-lived, the Lorentz force and the harmonic potential break the rotational symmetry in the coordinate space which eventually introduces additional J/ψ asymmetry at relatively large p_T ($\sim$ 10 GeV/c).

The results for Au+Au collisions at $\sqrt{s_{NN}}$ = 200 GeV recorded at RHIC in 2010 (Run10) have been published [13]. Since the publication, more data have been taken in 2011 (Run11). Our analysis utilized the Run11 dataset, which was then combined with Run10 results, in order to reduce the statistical uncertainty and hopefully achieve a stronger conclusion.

2. J/ψ reconstruction

In this analysis, the J/ψ particles were reconstructed via the $J/\psi \to e^+e^-$ channel, which has a branching ratio of 5.9%. Two daughter tracks of the J/ψ particles were required to have more than 20 space points in the Time Projection Chamber (TPC), and their distances of closest approach (DCA) less than 1 cm from the primary vertex. Low-momentum electrons and positrons can be separated from hadrons by applying a cut on the inverse velocity ($0.97 < 1/\beta < 1.03$), which was calculated from the time of flight measured by the Time-of-Flight detector, and the path length measured by the TPC. At larger momenta ($p > 1.5\,\mathrm{GeV}/c$), a cut on the momentum-to-energy ratio ($0.3 < p/E < 1.5$) was required to select electrons and positrons, where the energy was measured by the Barrel Electromagnetic Calorimeter. More than 15 TPC space points were required to calculate the energy loss ($\langle dE/dx \rangle$) inside the TPC. The electrons and positrons were further identified by their specific $\langle dE/dx \rangle$ with an asymmetric cut around the expected value, because the lower side has more hadron contamination. The cut also varies according to whether the candidate track passes the $1/\beta$ and/or p/E cut for efficiency optimization. With this combination of $1/\beta$, p/E and $\langle dE/dx \rangle$ cuts, we can identify electrons and positrons in a wide momentum range. The measured J/ψ particles cover the rapidity range $-1 < y < 1$, favoring J/ψ particles near $y = 0$ because of detection efficiency variation due to acceptance and decay kinematics.

3. Measuring J/ψ v_2

In our analysis, we obtained the J/ψ v_2 using event plane method [9]. Firstly, we divided the measurements of J/ψ yields into 10 bins in $(\phi - \Psi)$, ranging from 0 to π. ϕ is the azimuthal angle of J/ψ momentum in cylindrical coordinate system, and Ψ is the event plane angle obtained from the azimuthal distribution of TPC tracks. Two bins at supplementary angles were combined into one. For example, the bin at 0-0.1π and the bin at 0.9π-π were combined. Different event plane resolutions (R) were used for different centrality bins, as listed in Table 1. Entries in the invariant mass distribution of electron and positron pairs were weighted by 1/R according to the centrality [14].

Table 1. Event plane resolution (R) for different centralities.

Centrility(%)	0-5	5-10	10-20	20-30	30-40	40-50	50-60	60-70	70-80
R	0.360	0.478	0.613	0.727	0.798	0.360	0.793	0.695	0.555

Then the J/ψ yield within each combined $(\phi - \Psi)$ bin was obtained by fitting the weighted invariant mass distribution with a Crystal Ball function [15] as signal, sitting on top of a second-order polynomial function as background. The Crystal Ball function (see equation 1) consists

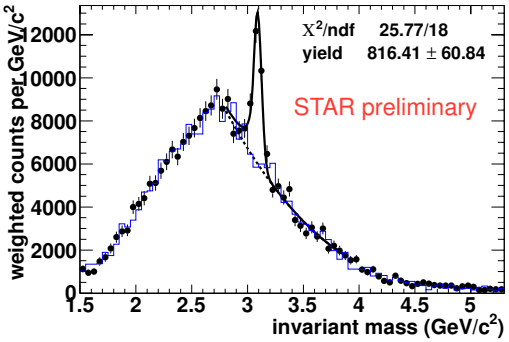

Figure 1. An example of obtaining J/ψ yield. ($0 < p_T < 2$ GeV/c, centrality 10-40% and $0.1\pi < \phi - \Psi < 0.2\pi$).

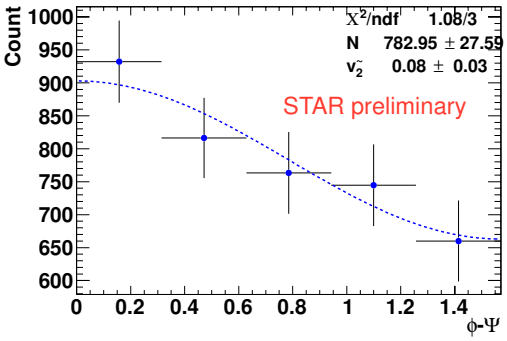

Figure 2. An example of obtaining J/ψ v_2 ($0 < p_T < 2$ GeV/c, centrality 10-40%).

of a Gaussian core and a power-law tail at low mass to account for the energy loss of electrons and J/ψ radiative decays.

$$f(x;\alpha,n,\bar{x},\sigma) = N \cdot \begin{cases} \exp\left(-\frac{(x-\bar{x})^2}{2\sigma^2}\right), & \text{for } \frac{x-\bar{x}}{\sigma} > -\alpha \\ \left(\frac{n}{|\alpha|}\right)^n \cdot \exp\left(-\frac{|\alpha|^2}{2}\right) \cdot \left(\frac{n}{|\alpha|} - |\alpha| - \frac{x-\bar{x}}{\sigma}\right)^{-n}, & \text{for } \frac{x-\bar{x}}{\sigma} \leq -\alpha \end{cases} \quad (1)$$

Fig. 1 is an example of e^+e^- invariant mass distribution and the corresponding fit for J/ψ peak in a selected bin. With yield obtained for each $(\phi - \Psi)$ bin, we extracted v_2 by fitting the J/ψ yield as a function of $(\phi - \Psi)$ with the function $y = N(1 + v_2 \cos[2(\phi - \Psi)])$, as shown in Fig. 2. Finally the observed v_2 was scaled by 1/R and $0.1\pi/\sin(0.1\pi)$ to correct for the event plane resolution and bin width effect, where 0.1π was the bin width of our $(\phi - \Psi)$ bins.

4. Combining Run10 and Run11 results

The same track selection and fitting method were used for both Run10 and Run11 analyses. The consistency of these two results has been checked by performing a so-called Z-test [16], as showed in Fig. 3. For each pair of points at a given p_T, their consistency can be quantified by $Z_i = (a_i - b_i)/\sqrt{s_{a_i}^2 + s_{b_i}^2}$, where a_i and b_i are the J/ψ v_2 extracted from Run10 and Run11 datasets, and s_{a_i} and s_{b_i} are the corresponding uncertainties. The value of each Z_i is small (< 2), therefore the difference between each pair is below 2σ. For two consistent datasets, the sum of Z_i should follow a normal distribution with the mean equal to 0 and the σ equal to $\sqrt{N}$, where N is the number of pairs. In our analysis, $N = 4$ and the $\sum Z_i$ is also below 2σ. Therefore we can safely combine the results of two runs and take their difference as a conservative estimate of the systematic uncertainty.

Fig. 4 shows the combined result of Run10 and Run11 analyses together with model calculations. It is noticeable that for p_T above 2 GeV/c, especially the second bin, our measured v_2 is consistent with zero. Based on the calculations of v_2 for J/ψ from the coalescence of thermalized charm quarks [7] and the possible non-flow contribution to the measured v_2, we can infer that in case the charm quarks are fully thermalized, the contribution of regeneration to J/ψ production above 2 GeV/c is unlikely to be the dominant source.

5. Summary

J/ψ v_2 from Run11 data has been obtained and combined with previous Run10 results. The combined result for Au+Au collisions at $\sqrt{s_{NN}} = 200$ GeV is presented as a function of J/ψ

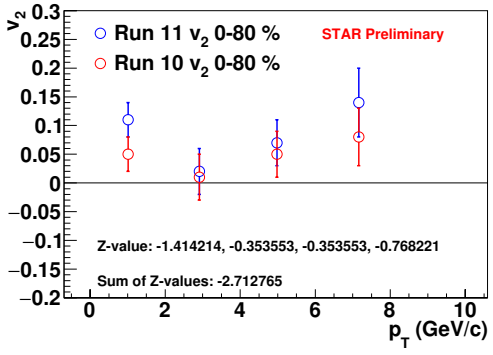

Figure 3. The Z-test of Run10 and Run11 results.

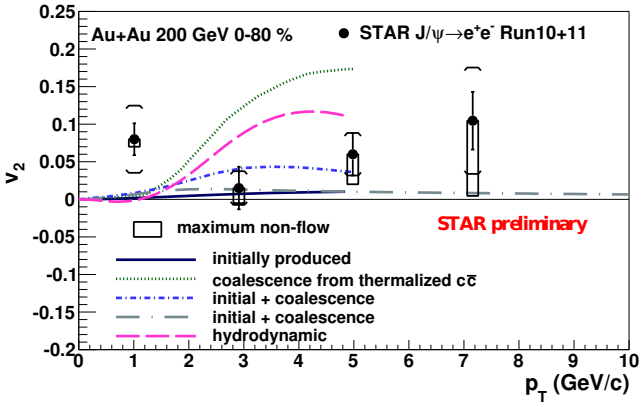

Figure 4. The combined result of Run10 and Run11.

transverse momentum. For p_T above 2 GeV/c, the measured v_2 is consistent with zero within statistical and systematic uncertainties. Comparing to model calculations, the measured v_2 disfavors the scenario that the dominant contribution to the observed yields at this kinematic region is the regeneration of fully thermalized charm quarks. Future work is needed to finalize the systematic uncertainties by comparing different fitting methods, studying trigger bias, etc.

Acknowledgments

This work was supported in part by National Natural Science Foundation of China under contract Nos. 11220101005 and 11421505, the Major State Basic Research Development Program in China under Contract No. 2014CB845401.

References

[1] Arsene I *et al.* (BRAHMS) 2005 *Nucl. Phys.* **A757** 1–27 (*Preprint* nucl-ex/0410020)
[2] Back B B *et al.* 2005 *Nucl. Phys.* **A757** 28–101 (*Preprint* nucl-ex/0410022)
[3] Adams J *et al.* (STAR) 2005 *Nucl. Phys.* **A757** 102–183 (*Preprint* nucl-ex/0501009)
[4] Adcox K *et al.* (PHENIX) 2005 *Nucl. Phys.* **A757** 184–283 (*Preprint* nucl-ex/0410003)
[5] Chatrchyan S *et al.* (CMS) 2012 *JHEP* **05** 063 (*Preprint* 1201.5069)
[6] Abelev B *et al.* (ALICE) 2012 *Phys. Rev. Lett.* **109** 072301 (*Preprint* 1202.1383)
[7] Greco V, Ko C M and Rapp R 2004 *Phys. Lett.* **B595** 202–208 (*Preprint* nucl-th/0312100)
[8] Ravagli L and Rapp R 2007 *Phys. Lett.* **B655** 126–131 (*Preprint* 0705.0021)
[9] Poskanzer A M and Voloshin S A 1998 *Phys. Rev.* **C58** 1671–1678 (*Preprint* nucl-ex/9805001)
[10] Yan L, Zhuang P and Xu N 2006 *Phys. Rev. Lett.* **97** 232301 (*Preprint* nucl-th/0608010)
[11] Liu Y, Xu N and Zhuang P 2010 *Nucl. Phys.* **A834** 317C–319C (*Preprint* 0910.0959)
[12] Guo X, Shi S, Xu N, Xu Z and Zhuang P 2015 *Phys. Lett.* **B751** 215–219 (*Preprint* 1502.04407)
[13] Adamczyk L *et al.* (STAR) 2013 *Phys. Rev. Lett.* **111** 052301 (*Preprint* 1212.3304)
[14] Masui H, Schmah A and Poskanzer A M 2016 *Nucl. Instrum. Meth.* **A833** 181–185 (*Preprint* 1212.3650)
[15] Gaiser J 1982 *Charmonium Spectroscopy From Radiative Decays of the J/ψ and ψ'* Ph.D. thesis SLAC
[16] Sprinthall R C 2011 *Basic statistical analysis* 9th ed (Pearson Education)